Volume 3 | Number 47 | 21 December 2015 | Pages 12167–12336

Journal of Materials Chemistry C

Materials for optical, magnetic and electronic devices

www.rsc.org/MaterialsC

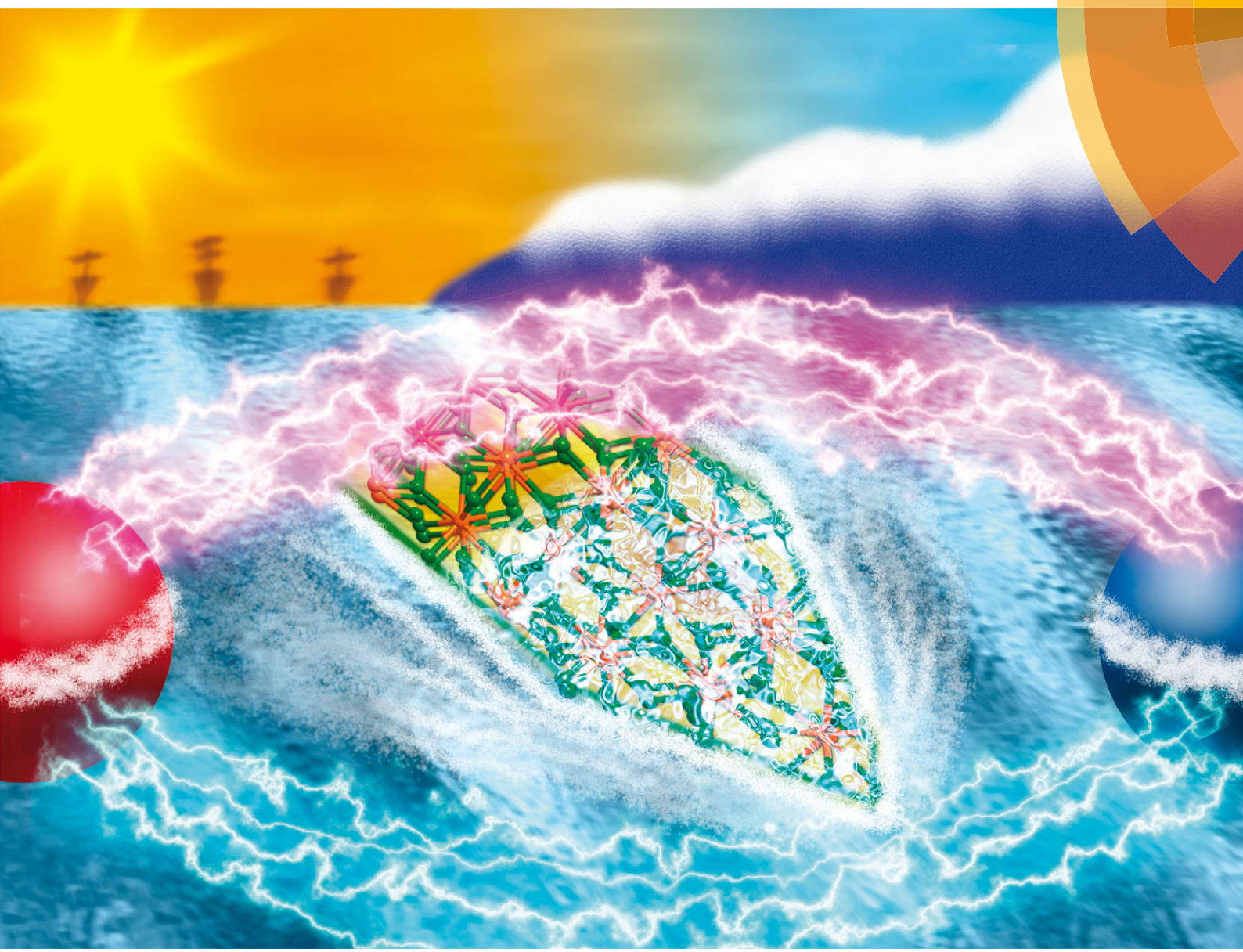

ISSN 2050-7526

ROYAL SOCIETY OF CHEMISTRY

PAPER

Jian-Hua Jia, Ming-Liang Tong *et al.*

A brilliant cryogenic magnetic coolant: magnetic and magnetocaloric study of ferromagnetically coupled GdF_3

Journal of Materials Chemistry C

PAPER

View Article Online
View Journal | View Issue

Cite this: J. Mater. Chem. C, 2015, 3, 12206

A brilliant cryogenic magnetic coolant: magnetic and magnetocaloric study of ferromagnetically coupled GdF_3†

Yan-Cong Chen,[a] Jan Prokleška,[b] Wei-Jian Xu,[a] Jun-Liang Liu,[a] Jiang Liu,[a] Wei-Xiong Zhang,[a] Jian-Hua Jia,*[a] Vladimír Sechovský[b] and Ming-Liang Tong*[a]

Received 30th July 2015,
Accepted 6th October 2015

DOI: 10.1039/c5tc02352a

www.rsc.org/MaterialsC

The use of paramagnetic molecules as cryogenic coolants usually requires relatively large fields to obtain a practical cooling effect. Thus, research into magnetic molecular materials with larger MCEs in fields of $\leq$2 T is the main focus in this area. In this work, the crystal structure, magnetic susceptibility and isothermal magnetization for the inorganic framework material GdF_3 were measured, and the isothermal entropy change was evaluated up to 9 T. Thanks to the combination of the large isotropic spin of Gd^{3+}, the dense structure and weak ferromagnetic interaction, an extremely large $-\Delta S_m$ for GdF_3 was observed up to 528 mJ cm^{-3} K^{-1} for $\Delta\mu_0 H$ = 9 T, proving it to be an exceptional cryogenic magnetic coolant.

Introduction

The magnetocaloric effect (MCE) was discovered in 1881 in metallic iron by Warburg,[1] and magnetic refrigeration soon became a powerful technique to obtain and maintain an ultra-low temperature by adiabatic demagnetization (ADR).[2,3] In the early stages, cryogenic magnetic coolants were mainly inorganic paramagnetic salts and oxides, such as $Gd_2(SO_4)_3{\cdot}8H_2O$ and $Gd_3Ga_5O_{12}$ (GGG).[4] In recent years, molecular materials suddenly emerged in this field as an unprecedented classification, and a lot of highly competitive 3d,[5–11] 3d–4f[12–21] and 4f-type[22–29] molecular magnetic coolants have been synthesized and characterized. Their distinct advantages, such as stoichiometric composition, monodispersity and modifiability, have provided researchers with a perfect platform to realize the design strategies towards cryogenic magnetic coolants. Various lessons have been learned and proved, including but not limited to, the large spin state, low anisotropy, weak interaction and large metal-to-ligand ratio.[30–35]

For the best cooling performance at around liquid helium temperature, it is believed that the Gd^{3+} ion is a wonderful choice owing to the half-filled 4f orbital (S = 7/2), magnetic isotropy and usually weak exchange interactions. Additionally, the low magnetic ordering temperature can still be maintained even with a high metal-to-ligand ratio, and a large MCE can be obtained, especially with volumetric units.[36,37] Soon after, the competition in molecular magnetic coolants became a race towards a reduction of the counterions accompanying Gd^{3+}. To date, many gadolinium carboxylates including acetates, formates and oxalates have been reported, with increasing MCE chasing after the performance of GGG.[38–42]

Since there is little room for organic ligands to keep shrinking, the most recent focus in this field dramatically returned to inorganic compounds based on small counterions such as OH^-, SO_4^{2-}, and O^{2-}.[43–45] Following the strategies learned for molecular systems,[30–35] significant enhancement of the MCE in these inorganic compounds has been observed, and orthorhombic $Gd(OH)CO_3$ finally surpassed the performance of GGG and set a new record.[46] However, the story seems to not be over yet, as a better example, $GdPO_4$, was reported after just half a year.[47]

In the inorganic area, the utilization of the aforementioned strategies must be more carefully applied, because strong magnetic interactions are more likely to exist, thus hindering the MCE. Compared with relatively versatile magnetic interactions through OH^-, SO_4^{2-}, and O^{2-} bridges, weak ferromagnetic coupling through bent μ-F^- bridges is often observed in lanthanide complexes,[48,49] which urged us to investigate the MCE performance of gadolinium fluoride. Although GdF_3 was tested as the working material for a toroidal ADR prototype,[50] the presence of a Gd_2O_3 impurity prevented the intrinsic magnetocaloric performance of GdF_3 from being revealed. Herein, we report the detailed magnetic and magnetocaloric study on a pure sample of GdF_3. The occurrence of ferromagnetic coupling and an extremely large MCE proves it to be the best cryogenic magnetic coolant ever reported.

[a] Key Laboratory of Bioinorganic and Synthetic Chemistry of Ministry of Education, School of Chemistry & Chemical Engineering, Sun Yat-Sen University, Guangzhou, 510275, China. E-mail: tongml@mail.sysu.edu.cn
[b] Faculty of Mathematics and Physics, Department of Condensed Matter Physics, Charles University, Ke Karlovu 5, CZ-12116 Prague 2, Czech Republic

† Electronic supplementary information (ESI) available: Additional crystallography tables and figures of magnetic properties. See DOI: 10.1039/c5tc02352a

Experimental section

Synthesis of GdF_3

Pure polycrystalline GdF_3 can be hydrothermally synthesized using the analytical reagent (>99.9%) aqueous $GdCl_3$ and an excess amount of $NaBF_4$ or NH_4F, while the commercial product is also available.

X-ray crystallography

The X-ray powder diffraction data for structure refinement was collected on a Bruker D8 Advance with a Cu K_α radiation source (40 kV, 40 mA). The step-scanned X-ray powder diffraction data was recorded in the 2θ range of 20–115° with 0.02° 2θ steps and 8 seconds per step scan speed. The structural model of TbF_3 (in space group *Pnma*) was used as the initial structural model for Rietveld refinement, which was carried out using the Reflex Powder Refinement module of Material Studio. The structural parameters, together with pseudo-Voigt profile parameters, background parameters, the cell constants, the zero point of the diffraction pattern, the Berar–Baldinozzi asymmetry correction parameters and the March–Dollase preferred orientation correction parameters, were optimized step by step to improve the agreement between the calculated and the experimental powder diffraction patterns. The final Rietveld refinement plot is shown in Fig. S1 (ESI†). Further details on the crystal structure may be obtained from the ESI† (Tables S1 and S2) and from the Fachinformationszentrum Karlsruhe, 76344 Eggenstein-Leopoldshafen, Germany (fax: (+49) 7247-808-666; e-mail: crysdata@fiz-karlsruhe.de), by quoting the depository number CSD-429920 (GdF_3).

Physical measurements

Magnetic measurements were performed on a polycrystalline sample of GdF_3 using a Quantum Design PPMS with VSM option. Variable-temperature magnetic susceptibility measurements were performed on a polycrystalline sample in an applied dc field of 0.1 T between 2–300 K, and the isothermal magnetization was measured from 2 K to 10 K in an applied dc field up to 9 T. A diamagnetic correction was applied based on Pascal's constant. The low-temperature specific heat was studied on a Quantum Design PPMS up to 9 T with the ^{3}He option adopting the standard relaxation technique.

Results and discussion

Crystal structure

Although the powder X-ray diffraction pattern of GdF_3 was listed in JCPDF #49-1804, the exact crystal structure has not been determined. Here, by Rietveld refinement on the powder X-ray diffraction pattern (Fig. S1, ESI†), it is found that GdF_3 crystallizes in the orthorhombic space group *Pnma* and shares the same structure as SmF_3, EuF_3, TbF_3, HoF_3 and YbF_3 (Table 1). In the crystal structure, each Gd^{3+} ion is 9-coordinated in a tricapped trigonal prismatic geometry (Fig. 1), while each F^- ion is μ_3-bridging, just corresponding to the stoichiometric ratio 1:3. The lengths of the Gd–F bonds are generally similar, ranging from 2.331 to 2.501 Å, while the Gd–F–Gd angles are quite different, lying between 98.88° and 139.03°. The nearest Gd···Gd separations are 3.672 Å, which form a series of zigzag chains along the *a* axis and then further extend into a 3-dimensional framework (Fig. 1 and Fig. S2, ESI†). Thanks to the simple composition, the formula mass of GdF_3 is only 214.25 g mol^{-1}, trapping as much as 73.4% of Gd^{3+} in an extremely dense structure with ρ = 7.062 g cm^{-3}. Therefore, GdF_3 shall be a wonderful magnetic coolant so long as there is no long-range antiferromagnetic ordering in the working temperature region.

Table 1 Crystal data and structural refinement for GdF_3

Chemical formula	GdF_3
Formula mass/g mol^{-1}	214.25
Crystal system	Orthorhombic
Space group	*Pnma*
Z	4
a/Å	6.5718(1)
b/Å	6.9844(1)
c/Å	4.3903(1)
Unit cell volume/Å^3	201.21
ρ_{calcd}/g cm^{-3}	7.062
R_p	1.62%
R_{wp}	2.21%

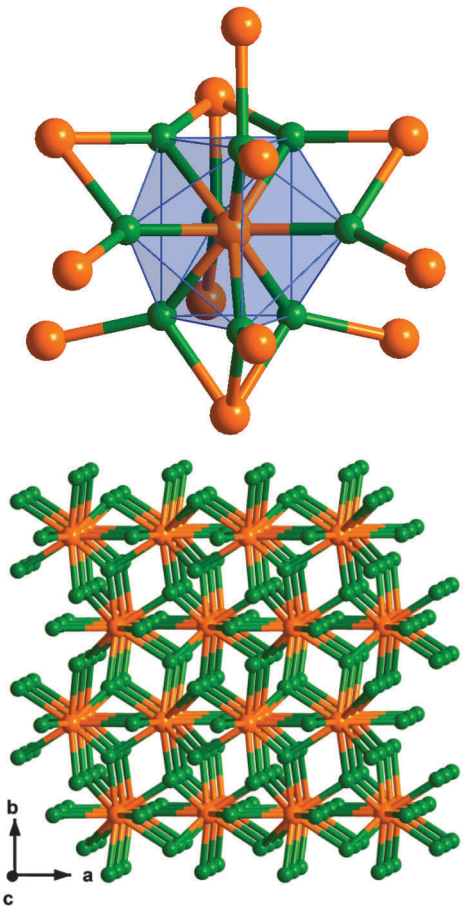

Fig. 1 The crystal structure of GdF_3. Top: The coordination environment of Gd^{3+}. Bottom: The extended framework of GdF_3 viewed along the *c* axis. Colour codes: Gd, orange; F, green.

Magnetic properties

Variable-temperature magnetic susceptibility measurements were performed on a polycrystalline sample of GdF_3 in an applied dc field of 0.1 T (Fig. 2). At room temperature, the $\chi_m T$ value is 7.96 cm^3 K mol^{-1}, slightly larger than the spin-only value expected for a free Gd^{3+} ion with $g = 2$ (7.875 cm^3 K mol^{-1}). Upon cooling, $\chi_m T$ kept increasing to 11.2 cm^3 K mol^{-1} at 2 K, suggesting dominant ferromagnetic interactions between the Gd^{3+} ions. The inverse magnetic susceptibility ($1/\chi_m$) obeys the Curie–Weiss law with $C = 7.91$ cm^3 K mol^{-1} and $\theta = +0.7$ K. No sign of the long-range magnetic ordering can be observed above 2 K, as the ordering temperature is reported to be around 1.25 K.[51] Such a behaviour is extremely favourable for a large cryogenic MCE, and it is quite different from those complexes with hydroxide bridges, where strong antiferromagnetic interactions are common and usually harm the full utilization of the MCE. The ferromagnetic coupling in GdF_3 and the low ordering temperature rule out our last worry about its capability as a promising cryogenic magnetic coolant.

To calculate the precise value of $-\Delta S_m$, the isothermal magnetization for GdF_3 was measured from 2 K to 10 K in an applied dc field up to 9 T (Fig. 2). The magnetization increases quickly with the applied field below 2 T and reaches a saturation value of 7.0 $N\beta$ at 2 K and 9 T, which is in good agreement with the expected value for a Gd^{3+} ion ($s = 7/2$, $g = 2$).

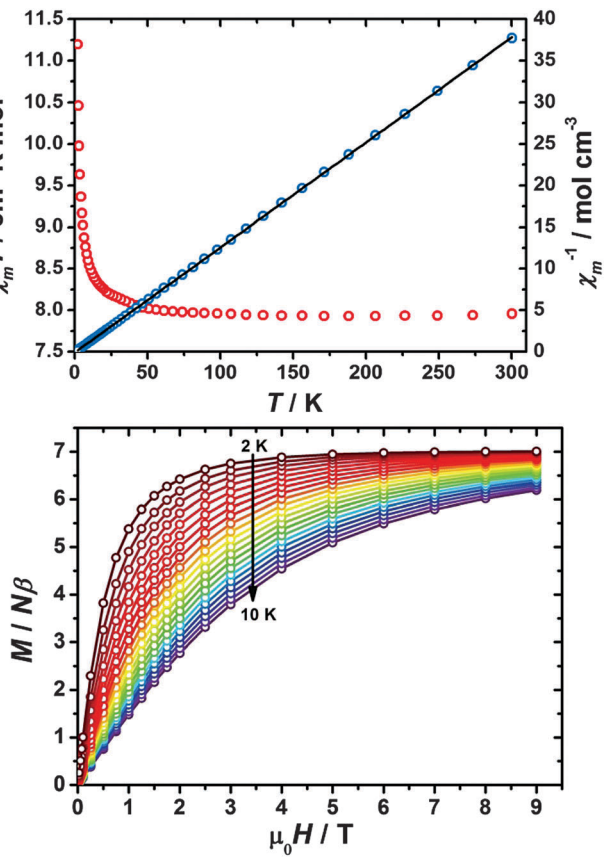

Fig. 2 Magnetic properties of GdF_3. Top: Temperature-dependencies of the magnetic susceptibility product ($\chi_m T$) and inverse magnetic susceptibility ($1/\chi_m$) at 2–300 K with a dc field of 0.1 T. Bottom: Magnetization *versus* the dc field in the temperature range of 2–10 K. The black solid line represents the least-square fit for the Curie–Weiss law.

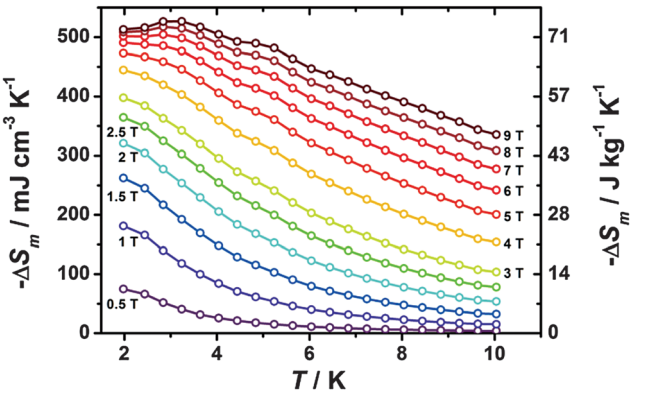

Fig. 3 Temperature-dependencies of $-\Delta S_m$ for selected values of $\Delta\mu_0 H$ obtained from magnetization data. The data with field variation below 0.5 T are omitted for clarity.

The isothermal entropy change can be calculated by applying the Maxwell equation:

$$\Delta S_m(T) = \int_0^H [\partial M(T,H)/\partial T]_H \mathrm{d}H$$

Just as for many reported ferromagnetic coupling systems, the maximum $-\Delta S_m$ values for GdF_3 grow rapidly with increasing ΔH, namely 181 mJ cm^{-3} K^{-1}, 321 mJ cm^{-3} K^{-1} and 399 mJ cm^{-3} K^{-1} for $\Delta\mu_0 H$ = 1 T, 2 T and 3 T, respectively (Fig. 3). For larger ΔH, the increase of $-\Delta S_m$ values become slower, reaching 474 mJ cm^{-3} K^{-1} and 506 mJ cm^{-3} K^{-1} for $\Delta\mu_0 H$ = 5 T and 7 T, and the peaks of the $-\Delta S_m$ *versus* T curves gradually shift to higher temperatures. These results are in line with the heat capacity tests for the toroidal ADR prototype,[51] and the maximum value we obtained here is 528 mJ cm^{-3} K^{-1} (74.8 J kg^{-1} K^{-1}) at T = 3.2 K and $\Delta\mu_0 H$ = 9 T, close to the theoretical limiting value of 570 mJ cm^{-3} K^{-1} (80.7 J kg^{-1} K^{-1}) calculated from $R\ln(2s+1)/M_w$ with $s = 7/2$ and M_w = 214.25 g mol^{-1}.

Heat capacity

The low temperature heat capacity (C) measurements were also performed to further investigate the MCE of GdF_3 (Fig. 4), and no peak around 3.8 K corresponding to Gd_2O_3 can be found.[50] The curves show typical trends to those of most cryogenic magnetic coolants, with the higher temperature region attributed to the lattice contribution and the lower part dominated by a Schottky type magnetic contribution. The lattice one, C_{latt}, can be fitted to the Debye's model and yield a high Debye temperature (θ_D) of 284(3) K with $r_D = 4$, indicating a rigid crystal framework that is favourable to a large MCE. A λ-shaped anomaly is observed in the zero field at approximately 1.21 K but is suppressed by applied fields, indicating the emergence of a magnetic phase transition in good agreement with the reported 1.25 K.[51]

Then, the entropy can be obtained by numerical integration from the experimental C, using:

$$S(T) = \int_0^T C(T)/T \mathrm{d}T$$

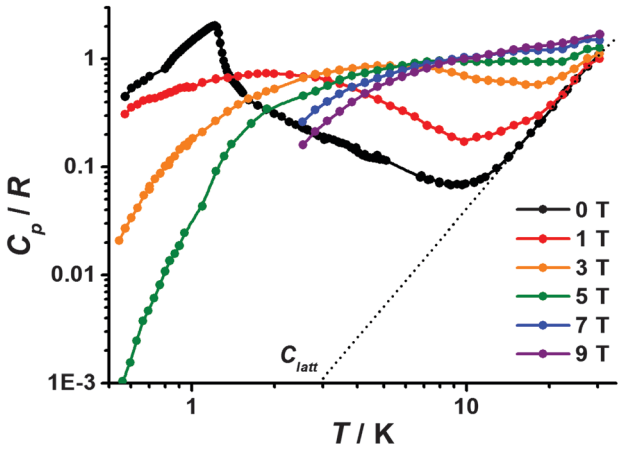

Fig. 4 Temperature-dependencies of the heat capacity normalized to the gas constant in selected applied fields. The dotted line represents the lattice contribution.

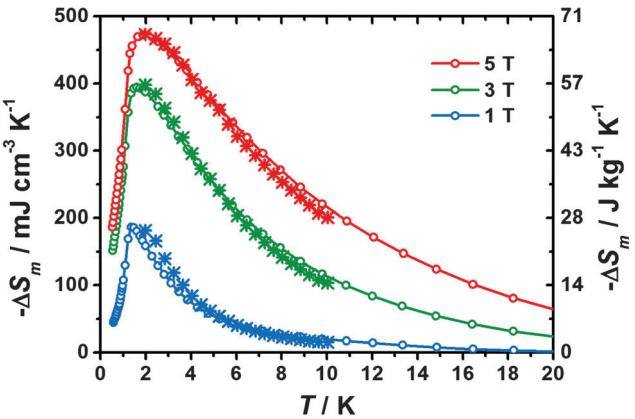

Fig. 5 Temperature-dependencies of $-\Delta S_m$ obtained from magnetization (★) and heat capacity (●) for selected $\Delta\mu_0 H$.

with a constant value based on the high temperature saturation value of magnetic entropy ($S_{m,sat} = R\ln(2s + 1) = 2.08R$) added to the low-field entropy to compensate for experimental inaccessibility to absolute zero. From the heat capacity, the maximal isothermal magnetic entropy changes (ΔS_m) were obtained as 186 mJ cm^{-3} K^{-1}, 395 mJ cm^{-3} K^{-1} and 473 mJ cm^{-3} K^{-1} for $\Delta\mu_0 H$ = 1 T, 3 T and 5 T, respectively, in great agreement with the results calculated from the magnetization (Fig. 5). These are accompanied by the large adiabatic temperature change (ΔT_{ad}) up to 17 K for $\Delta\mu_0 H$ = 5 T (Fig. S3, ESI†), highlighting the competitiveness of GdF_3 as a brilliant cryogenic magnetic coolant.

Conclusions

The area of cryogenic magnetic coolants is full of competition, and there has never been a candidate that can hold the record for a long time. Thanks to such competition in a sense, researchers are now much wiser at adopting suitable strategies for the design of high performance magnetic coolants. Although the record set by $Gd(OH)CO_3$[46] has been overtaken recently, we

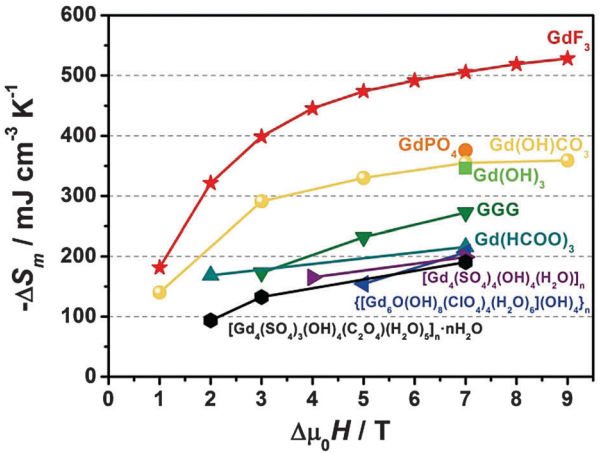

Fig. 6 The maximum reported $-\Delta S_m$ value *versus* the corresponding $\Delta\mu_0 H$ for selected cryogenic magnetic coolants.

Table 2 Magnetic entropy changes for selected molecule-based materials

Complex[ref.]	$\Delta\mu_0 H$ (T)	$-\Delta S_{m,max}$ (J kg^{-1} K^{-1})	$-\Delta S_{m,max}$ (mJ cm^{-3} K^{-1})
$[Gd_4(SO_4)_3(OH)_4(C_2O_4)(H_2O)_5]_n \cdot nH_2O$[45]	7	51.5	190
$[Gd_4(SO_4)_4(OH)_4(H_2O)]_n$[44]	7	51.3	199
$\{[Gd_6O(OH)_8(ClO_4)_4(H_2O)_6](OH)_4\}_n$[43]	7	46.6	207
$Gd(HCOO)_3$[41]	7	55.9	216
$Gd_3Ga_5O_{12}$ (GGG)[4]	7	38.4	272
$Gd(OH)_3$[52]	7	62.0	346
$Gd(OH)CO_3$[46]	7	66.4	355
$GdPO_4$[47]	7	62.0	376
GdF_3 (this work)	2	45.5	321
	5	67.1	474
	7	71.6	506

haven't stopped searching and finally, present ferromagnetically coupled GdF_3.

As demonstrated in Fig. 6 and Table 2, another cryogenic magnetic coolant with $-\Delta S_m$ larger than 400 mJ cm^{-3} K^{-1} has never been reported, while the maximum value for GdF_3 has already exceeded 500 mJ cm^{-3} K^{-1}. Comparing the $-\Delta S_m$ with $\Delta\mu_0 H$ = 7 T for the sake of fairness, the performance of GdF_3 (506 mJ cm^{-3} K^{-1}) surpasses that of $GdPO_4$ (375.8 mJ cm^{-3} K^{-1})[47] by 34.6%, setting a new record. Last but not least, the dense structure and ferromagnetic interaction in GdF_3 still leads to an excellent performance, even for lower $\Delta\mu_0 H$ such as 2 T and 1 T, highlighting its competitiveness.

At this point, we believe that the long journey in pursuit of the best cooling performance is close to the extreme. There is limited room, if any, for a further increase in the $-\Delta S_m$ value itself for Gd-based materials: some other compounds like GdOF, GdOOH, $GdBO_3$ and $Gd_2(CO_3)_3$ might be worth investigating, while Gd_2O_3 and $Gd(OH)_3$[52] are already known as antiferromagnets and suffer from a severe decrease in the full entropy. Future study on the cryogenic MCE shall turn the focus onto the other parameters such as ΔT_{ad}, cooling power and even production cost, where the Mn-based materials become strong competitors.[11] Although we have to admit that the coordination complexes with organic ligands

can never be so comparative with inorganic complexes in such a sense, it should not be forgotten that the ambitions of molecular materials have never been just about the value. We have witnessed how numerous complexes that seem useless can be rationally modified into good candidates for magnetic coolants, and we have been continuously learning about the magneto-structural correlations during the design and synthesis of these complexes. Furthermore, the chemists' powerful skills in material engineering can still help to modify the behaviour of inorganic compounds in the limitless fields of nanomaterials and organic–inorganic hybrid materials, where the magnetic interaction, ordering temperature and low-field performance may be fine-tuned and optimized. *It is, perhaps, the end of the beginning.*

Acknowledgements

This work was supported by the "973 Project" (2012CB821704 and 2014CB845602), project NSFC (Grant no. 91122032, 21371183, 21121061 and 21201137), the NSF of Guangdong (S2013020013002), Program for Changjiang Scholars and Innovative Research Team in the University of China (IRT1298). Some of the thermodynamic studies were performed at MLTL (http://mltl.eu/), which is supported within the program of Czech Research Infrastructures (project no. LM2011025).

Notes and references

1 E. Warburg, *Ann. Phys.*, 1881, **249**, 141.
2 P. Debye, *Ann. Phys.*, 1926, **386**, 1154.
3 W. F. Giauque, *J. Am. Chem. Soc.*, 1927, **49**, 1864.
4 B. Baudun, R. Lagnier and B. Salce, *J. Magn. Magn. Mater.*, 1982, **27**, 315.
5 M. Manoli, R. D. L. Johnstone, S. Parsons, M. Murrie, M. Affronte, M. Evangelisti and E. K. Brechin, *Angew. Chem., Int. Ed.*, 2007, **119**, 4540.
6 M. Manoli, A. Collins, S. Parsons, A. Candini, M. Evangelisti and E. K. Brechin, *J. Am. Chem. Soc.*, 2008, **130**, 11129.
7 S. Nayak, M. Evangelisti, A. K. Powell and J. Reedijk, *Chem. – Eur. J.*, 2010, **16**, 12865.
8 J.-P. Zhao, R. Zhao, Q. Yang, B.-W. Hu, F.-C. Liu and X.-H. Bu, *Dalton Trans.*, 2013, **42**, 14509.
9 R. Shaw, R. H. Laye, L. F. Jones, D. M. Low, C. Talbot-Eeckelaers, Q. Wei, C. J. Milios, S. Teat, M. Helliwell, J. Raftery, M. Evangelisti, M. Affronte, D. Collison, E. K. Brechin and E. J. L. McInnes, *Inorg. Chem.*, 2007, **46**, 4968.
10 C.-B. Tian, R.-P. Chen, C. He, W.-J. Li, Q. Wei, X.-D. Zhang and S.-W. Du, *Chem. Commun.*, 2014, **50**, 1915.
11 Y.-C. Chen, J.-L. Liu, J.-D. Leng, F.-S. Guo, P. Vrábel, M. Orendáč, J. Prokleška, V. Sechovský and M.-L. Tong, *Chem. – Eur. J.*, 2014, **20**, 3029.
12 G. Karotsis, M. Evangelisti, S. J. Dalgarno and E. K. Brechin, *Angew. Chem., Int. Ed.*, 2009, **48**, 9928.
13 G. Karotsis, S. Kennedy, S. J. Teat, C. M. Beavers, D. A. Fowler, J. J. Morales, M. Evangelisti, S. J. Dalgarno and E. K. Brechin, *J. Am. Chem. Soc.*, 2010, **132**, 12983.
14 S. K. Langley, N. F. Chilton, B. Moubaraki, T. Hooper, E. K. Brechin, M. Evangelisti and K. S. Murray, *Chem. Sci.*, 2011, **2**, 1166.
15 Y.-Z. Zheng, M. Evangelisti and R. E. P. Winpenny, *Angew. Chem., Int. Ed.*, 2011, **50**, 3692.
16 J.-B. Peng, Q.-C. Zhang, X.-J. Kong, Y.-P. Ren, L.-S. Long, R.-B. Huang, L.-S. Zheng and Z. Zheng, *Angew. Chem., Int. Ed.*, 2011, **50**, 10649.
17 T. N. Hooper, J. Schnack, S. Piligkos, M. Evangelisti and E. K. Brechin, *Angew. Chem., Int. Ed.*, 2012, **51**, 4633.
18 Y.-Z. Zheng, M. Evangelisti, F. Tuna and R. E. P. Winpenny, *J. Am. Chem. Soc.*, 2012, **134**, 1057.
19 J.-B. Peng, Q.-C. Zhang, X.-J. Kong, Y.-Z. Zheng, Y.-P. Ren, L.-S. Long, R.-B. Huang, L.-S. Zheng and Z. Zheng, *J. Am. Chem. Soc.*, 2012, **134**, 3314.
20 E. M. Pineda, F. Tuna, R. G. Pritchard, A. C. Regan, R. E. P. Winpenny and E. J. L. McInnes, *Chem. Commun.*, 2013, **49**, 3522.
21 F.-S. Guo, Y.-C. Chen, J.-L. Liu, J.-D. Leng, Z.-S. Meng, P. Vrábel, M. Orendáč and M.-L. Tong, *Chem. Commun.*, 2012, **48**, 12219.
22 R. J. Blagg, F. Tuna, E. J. L. McInnes and R. E. P. Winpenny, *Chem. Commun.*, 2011, **47**, 10587.
23 R. Sibille, T. Mazet, B. Malaman and M. François, *Chem. – Eur. J.*, 2012, **18**, 12970.
24 M. Wu, F. Jiang, X. Kong, D. Yuan, L. Long, S. A. Al-Thabaiti and M. Hong, *Chem. Sci.*, 2013, **4**, 3104.
25 J.-M. Jia, S.-J. Liu, Y. Cui, S.-D. Han, T.-L. Hu and X.-H. Bu, *Cryst. Growth Des.*, 2013, **13**, 4631.
26 S. Biswas, A. Adhikary, S. Goswami and S. Konar, *Dalton Trans.*, 2013, **42**, 13331.
27 L.-X. Chang, G. Xiong, L. Wang, P. Cheng and B. Zhao, *Chem. Commun.*, 2013, **49**, 1055.
28 Y.-C. Chen, F.-S. Guo, Y.-Z. Zheng, J.-L. Liu, J.-D. Leng, R. Tarasenko, M. Orendáč, J. Prokleška, V. Sechovský and M.-L. Tong, *Chem. – Eur. J.*, 2013, **19**, 13504.
29 F.-S. Guo, Y.-C. Chen, L.-L. Mao, W.-Q. Lin, J.-D. Leng, R. Tarasenko, M. Orendáč, J. Prokleška, V. Sechovský and M.-L. Tong, *Chem. – Eur. J.*, 2013, **19**, 14876.
30 Yu. I. Spichkin, A. K. Zvezdin, S. P. Gubin, A. S. Mischenko and A. M. Tishin, *J. Phys. D: Appl. Phys.*, 2001, **34**, 1162.
31 M. Evangelisti and E. K. Brechin, *Dalton Trans.*, 2010, **39**, 4672.
32 R. Sessoli, *Angew. Chem., Int. Ed.*, 2012, **51**, 43.
33 J. W. Sharples and D. Collison, *Polyhedron*, 2013, **54**, 91.
34 Y.-Z. Zheng, G.-J. Zhou, Z. Zheng and R. E. P. Winpenny, *Chem. Soc. Rev.*, 2013, **43**, 1462.
35 J.-L. Liu, Y.-C. Chen, F.-S. Guo and M.-L. Tong, *Coord. Chem. Rev.*, 2014, **281**, 26.
36 K. A. Gschneidner, Jr. and V. K. Pecharsky, *Annu. Rev. Mater. Sci.*, 2000, **30**, 387.
37 K. A. Gschneidner, Jr., V. K. Pecharsky and A. O. Tsokol, *Rep. Prog. Phys.*, 2005, **68**, 1479.
38 M. Evangelisti, O. Roubeau, E. Palacios, A. Camín, T. N. Hooper, E. K. Brechin and J. J. Alonso, *Angew. Chem., Int. Ed.*, 2011, **50**, 6606.
39 F.-S. Guo, J.-D. Leng, J.-L. Liu, Z.-S. Meng and M.-L. Tong, *Inorg. Chem.*, 2012, **51**, 405.

40 G. Lorusso, M. A. Palacios, G. S. Nichol, E. K. Brechin, O. Roubeau and M. Evangelisti, *Chem.Commun.*, 2012, **48**, 7592.
41 G. Lorusso, J. W. Sharples, E. Palacios, O. Roubeau, E. K. Brechin, R. Sessoli, A. Rossin, F. Tuna, E. J. L. McInnes, D. Collison and M. Evangelisti, *Adv. Mater.*, 2013, **25**, 4653.
42 R. Sibille, E. Didelot, T. Mazet, B. Malaman and M. François, *APL Mater.*, 2014, **2**, 124402.
43 Y.-L. Hou, G. Xiong, P.-F. Shi, R.-R. Cheng, J.-Z. Cui and B. Zhao, *Chem. Commun.*, 2013, **49**, 6066.
44 S.-D. Han, X.-H. Miao, S.-J. Liu and X.-H. Bu, *Inorg. Chem. Front.*, 2014, **1**, 549.
45 S.-D. Han, X.-H. Miao, S.-J. Liu and X.-H. Bu, *Chem. – Asian J.*, 2014, **9**, 3116.
46 Y.-C. Chen, L. Qin, Z.-S. Meng, D.-F. Yang, C. Wu, Z. Fu, Y.-Z. Zheng, J.-L. Liu, R. Tarasenko, M. Orendáč, J. Prokleška, V. Sechovský and M.-L. Tong, *J. Mater. Chem. A*, 2014, **2** 9851.
47 E. Palacios, J. A. Rodríguez-Velamazán, M. Evangelisti, G. J. McIntyre, G. Lorusso, D. Visser, L. J. de Jongh and L. A. Boatner, *Phys. Rev. B: Condens. Matter Mater. Phys.*, 2014, **90**, 214423.
48 Q. Zhou, F. Yang, D. Liu, Y. Peng, G. Li, Z. Shi and S. Feng, *Inorg. Chem.*, 2012, **51**, 7529–7536.
49 K. S. Pedersen, M. A. Sørensen and J. Bendix, *Coord. Chem. Rev.*, 2015, **299**, 1–21.
50 M. DiPirro, E. Canavan, P. Shirron and J. Tuttle, *Cryogenics*, 2004, **44**, 559.
51 T. E. Katila, V. K. Typpi and G. K. Shenoy, *Solid State Commun.*, 1972, **11**, 1147.
52 Y. Yang, Q.-C. Zhang, Y.-Y. Pan, L.-S. Long and L.-S. Zheng, *Chem. Commun.*, 2015, **51**, 7317.